JOURNAL OF GEOPHYSICAL RESEARCH, VOL. 101, NO. A3, PAGES 5239–5249, MARCH 1, 1996

# Temporal and spatial variations in upper atmospheric $Mg^+$

J. Joiner[1] and A. C. Aikin

Laboratory for Atmospheres, NASA Goddard Space Flight Center, Greenbelt, Maryland

**Abstract.** Long-term behavior of magnesium ions in the upper atmosphere has been observed at wavelengths near 2800 Å using the Nimbus 7 solar backscattered ultraviolet (SBUV) instrument. Observations were made in the continuous spectral scan mode that operated approximately once a month from 1979 to 1986. Total column abundance of $Mg^+$ near local noon is the quantity derived from the nadir-viewing SBUV observations. $Mg^+$ total column abundances vary as a function of magnetic activity, solar sunspot activity, season, dip latitude, and longitude, as the result of changes in chemistry and ion transport. Increased $Mg^+$ column abundances are observed during periods of high magnetic activity at all latitudes. Total $Mg^+$ column abundances are observed to increase with solar sunspot activity at low and middle latitudes. Seasonal variation in the midlatitude $Mg^+$ column abundance is observed with a maximum near summer solstice. The total column abundances derived here are complementary to previous metallic ion studies in the upper $E$ and $F$ regions.

## Introduction

Because metallic ions have a long lifetime in the upper $E$ and $F$ regions against recombination with electrons, they act as passive tracers that aid in the understanding of upper atmosphere motions and ion transport mechanisms. Meteoric ablation near an altitude of about 100 km and sputtering of micrometeorites above 120 km are the sources of upper atmospheric metallic species, including magnesium. Metallic ions can be formed on impact and are also produced by charge exchange of neutral metals with major ionospheric species and direct photoionization. Metallic ions are transported upward into the upper $E$ and $F$ regions and above (altitudes from 120 km to several hundred kilometers) by different mechanisms dependent on latitude and altitude. $Mg^+$ is removed by radiative recombination in the upper $E$ and $F$ regions and in the lower $E$ region by the formation of $MgO_2{}^+$ and $MgO^+$ that recombines dissociatively to form neutral Mg. Correlations have been shown between upper atmospheric $Mg^+$ and other metallic ions [e.g., *Kumar and Hanson*, 1980; *Gardner et al.*, 1994], indicating that $Mg^+$ can be used to track metallic ionic species.

The first observation of ionized magnesium dayglow near 2800 Å was reported by *Anderson and Barth* [1971]. Subsequently, information about the altitude distribution of $Mg^+$, as well as other neutral metals and metallic ions in the $E$ region, has been obtained by use of rocket-borne mass spectrometers [e.g., *Aikin and Goldberg*, 1973; *Narcisi*, 1973]. In addition to information about the altitude distribution of neutral and ionized metals in the $E$ region, ground-based lidar also provides information about seasonal variations [e.g., *Gardner et al.*, 1993; *Kane and Gardner*, 1993]. Temporal and spatial variations in $Mg^+$ and other metallic ions in the upper $E$ and $F$ regions have been observed with zenith and limb-viewing radiometers, as well as with ion mass spectrometers and retarding potential analyzers flying on orbiting platforms [e.g., *Hanson et al.*, 1972; *Gerard and Monfils*, 1974, 1978; *Gerard* 1976; *Grebowsky and Brinton*, 1978; *Gerard et al.*, 1979; *Kumar and Hanson*, 1980; *Fesen and Hays*, 1982; *Mende et al.*, 1985; *Grebowsky and Reese*, 1989; *Gardner et al.*, 1994, 1995].

In this paper, we describe observations of $Mg^+$ dayglow near 2800 Å and infrequent detection of neutral Mg dayglow near 2850 Å using the Nimbus 7 solar backscattered ultraviolet (SBUV) instrument. Daytime, nadir-viewing backscattered ultraviolet (buv) observations have not been previously exploited as a means of measuring the abundance of $Mg^+$ in the upper atmosphere, although $Mg^+$ dayglow in SBUV observations has been noted by *Park et al.* [1986]. Our observations provide global coverage approximately once per month of the $Mg^+$ total column with a single instrument spanning a longer time period (1979-1986) than

[1] Also at Hughes STX Corporation, Greenbelt, Maryland.



Paper number 95JA03517.
0148-0227/96/95JA-03517$05.00

most previous metallic ion observations. Unlike many satellites from which metallic ion measurements have been made, the Nimbus 7 satellite was in a stable Sun-synchronous polar orbit during this time period. Therefore the SBUV observations provide a consistent time series of snapshots of the total $Mg^+$ column near local noon during different seasons and over approximately half of an 11-year solar cycle. The stability of the Sun-synchronous Nimbus 7 orbit and the nadir-viewing geometry of SBUV prevent the detection of diurnal and altitude variation in the $Mg^+$ distribution.

In the next section, we describe how the total column abundance of $Mg^+$ is retrieved from resonance scattering in satellite buv measurements. Next, variations in the $Mg^+$ total column abundance are shown as a function of magnctic activity, solar sunspot activity, season, dip latitudc, and longitudc. We compare our derived total $Mg^+$ column amounts qualitatively with previous upper $E$ and $F$ region metallic ion observations. Observed variations in $Mg^+$ total column amounts are then placed in context with the current understanding of metallic ion chemistry and transport mechanisms. In the last section, suggestions for future research are given.

## Determination of Column Abundance From SBUV Observations

The SBUV instrument flew on the Nimbus 7 satellite and operated reliably from 1979 to 1986. The SBUV instrument is a nadir-viewing double monochromator that measures backscattered solar radiation at wavelengths in the range 2000-4000 Å [*Heath et al.*, 1975; *Schlesinger et al.*, 1988]. Between 1979 and 1986, approximately 1 day per month was devoted to obtaining continuous spectral coverage of the Earth from 2000-4000 Å with a spectral resolution of 11.3 Å and a wavelength spacing of approximately 2 Å. A total of approximately 36,000 spectral scans were made on more than 114 separate days. Spectral scan observations of the solar irradiance were also made on or near the same days as the continuous spectral scan Earth observations.

The Nimbus 7 satellite had a stable Sun-synchronous polar orbit from 1979 to 1986 with an equatorial crossing time near local noon. On the ascending node of the orbit, the local time of observations varies with latitude by less than an hour about local noon. Approximately 20% of the scans at latitudes greater than 70° were obtained on the descending node of the orbit (observations near local midnight) in the summer hemisphere during sunlit conditions. In order to ensure that all reported observations were obtained at approximately the same local time, data from descending nodes are not used. However, when we examined the effect of including descending node data in our analysis, we found that the effect was insignificant.

Figure 1a shows an example of observed and computed radiances normalized to unit solar flux. Figure 1b shows the ratio of the observed to computed radiance, where the excess radiance at 280 nm (2800 Å) is clearly shown. Excess radiance near 2850 Å and 2800 Å can be attributed to two sources: (1) the filling-in effect (also known as the Ring effect) caused by rotational-Raman scattering (henceforth referred to as RRS) and (2) resonance scattering from $Mg^+$ or the neutral. The filling-in of solar Fraunhofer lines as the result of rotational-

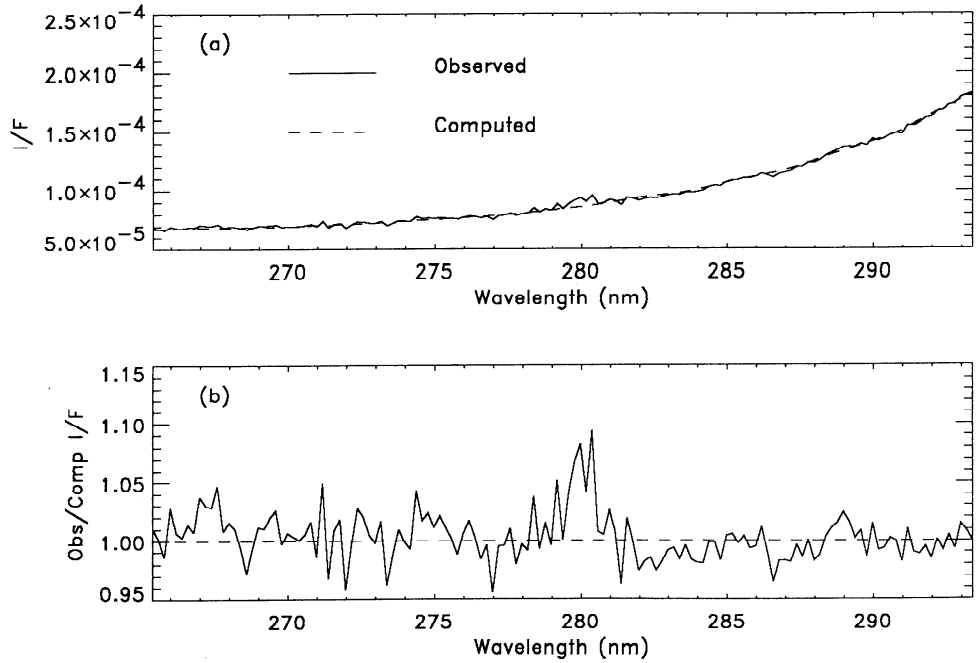


**Figure 1.** (a) Observed and computed ratio of radiance $I$ to solar irradiance $F$ versus wavelength for a single scan with solar zenith angle of 76°. (b) Ratio of observed to computed $I/F$.

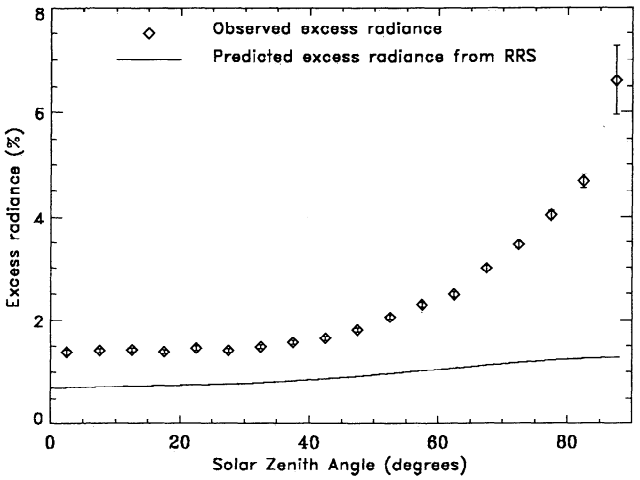


**Figure 2.** Observed excess radiance near 2800 Å in percent, averaged in 5° solar zenith angle bins with standard errors and the computed excess radiance expected from rotational-Raman scattering (RRS).

Raman scattering has been successfully modeled by *Joiner et al.* [1995]. The magnitude and solar zenith angle dependence of the excess radiance near the 2850-Å neutral Mg Fraunhofer line was found to be entirely consistent with that expected from RRS. Figure 2 shows a similar analysis of the excess radiance near the 2800-Å $Mg^+$ Fraunhofer line. The magnitude of the excess radiance and dependence on solar zenith angle cannot be explained by rotational-Raman scattering alone. Therefore resonance scattering by magnesium ions must be a significant source of the excess radiance.

In contrast with previous twilight $Mg^+$ dayglow observations using zenith- or limb-viewing spectrometers, most of the observed radiance in a nadir-viewing buv measurement is from the backscattered continuum. Resonance scattering by metallic ions against a continuum has also been observed in other planets [e.g., *Noll et al.*, 1995]. The total observed radiance, $I_{obs}$, in a buv measurement is given by

$$I_{obs} = I_b + I_{RRS} + I_{Mg}, \quad (1)$$

where $I_b$ is the backscattered continuum (set by Rayleigh scattering and ozone absorption), $I_{RRS}$ is the excess radiance from rotational-Raman scattering, and $I_{Mg}$ is the radiance from resonance scattering from $Mg^+$ or neutral Mg. In order to derive $I_{Mg}$, both $I_b$ and $I_{RRS}$ must be accurately modeled. $I_b$ can be computed using a single scattering model in which ozone is the only absorber. This is the model used to compute the radiance shown in Figure 1. When the single scattering calculation was performed, a small bias remained between the observed and computed radiances, probably the result of small errors in the SBUV calibration. In order to remove the bias, a different approach was employed to approximate $I_b$. A simple approximation of $I_b$ can be made by noting that the ozone cross section and thus $I_b$, normalized to unit solar irradiance, is a smooth function of wavelength at wavelengths shorter than 2900 Å. In order to model $I_b$, a second-order polynomial was fit to the normalized $I_{obs}$ at wavelengths between 2785 and 2860 Å not affected by RRS and/or $Mg^+$ or neutral Mg emission. The resulting continuum was nearly identical to that computed using a single scattering radiative transfer model, but the small bias between the observed and computed radiances was removed. The use of this technique also limits the effects of time-dependent calibration errors. $I_{RRS}$ was computed according to the *Joiner et al.* [1995] model. Then, $I_{Mg} = I_{ob} - I_b - I_{RRS}$ was converted to Rayleighs per angstrom and integrated over the appropriate wavelength band to yield the total emission in Rayleighs.

The only quantity that can be derived from the nadir-viewing SBUV radiances is the total column abundance below the satellite altitude of 955 km and above an altitude $z_0 \simeq 70$ km determined by ozone absorption at 2800 Å. Metallic ion density has been shown to decrease rapidly below 90 km based on rocket-borne mass spectrometer measurements [*Narcisi*, 1973] and chemical modeling [*Kane and Gardner*, 1993]. Therefore resonance scattering from below 70 km should be negligible.

The $Mg^+$ column abundance $\eta$, in ions per square centimeter, is related to the emission in Rayleighs, $4\pi J$, by

$$4\pi J = g\eta/\mu = g/\mu \int_{z_0}^{955\ \mathrm{km}} [Mg^+]\, dz, \quad (2)$$

where $\mu$ is the slant path correction ($\mu = 1$ for nadir observations), $g$ is the column emission rate, and $z$ is altitude. For the unresolved $Mg^+$ doublet, $g$ is given by

$$g = \frac{\pi e}{mc^2}\left[F_{(1/2,1/2)}\lambda^2_{(1/2,1/2)}f_{(1/2,1/2)} + F_{(3/2,1/2)}\lambda^2_{(3/2,1/2)}f_{(3/2,1/2)}\right], \quad (3)$$

where $e$, $m$, and $c$ have their usual meanings; the subscripts (1/2, 1/2) and (3/2, 1/2) refer to the $3s\ ^2S_{1/2} - 3p\ ^2P_{1/2}$ and $3s\ ^2S_{1/2} - 3p\ ^2P_{3/2}$ transitions at 2802.7 and 2795.5 Å, respectively; and for the appropriate transitions, $F$ is the solar irradiance, $\lambda$ is wavelength, and $f$ is the oscillator strength. A similar expression can be obtained for the $3s^2\ ^1S_0 - 3s3p\ ^1P_1$ transition of neutral Mg at 2852.1 Å. The oscillator strengths $f$ are 0.313 and 0.627 for the (1/2,1/2) and (1/2,3/2) $Mg^+$ transitions, respectively, and 1.6 for the neutral Mg transition [*Wiese et al.*, 1966].

The solar flux at the core of the $Mg^+$ unresolved doublet varies over both the solar rotational 27-day period and the 11-year solar cycle [e.g., *Heath and Schlesinger*, 1986]. We have accounted for this variation by making use of SBUV solar irradiance measurements on or near the same days as the continuous scan observations. This effect has not been accounted for in the analysis of previous $Mg^+$ dayglow observations. The SBUV instrument is not able to resolve the Mg doublet in the solar spectrum. Therefore we used high-resolution balloon

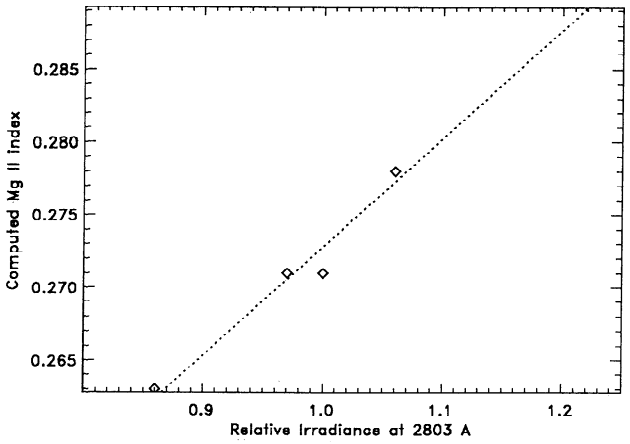


**Figure 3.** Computed solar backscatter ultraviolet Mg II index as a function of the 2803-Å solar irradiance relative to that measured in 1981 for four available high-spectral-resolution solar irradiance measurements (diamonds) and least squares linear fit (dotted line).

solar irradiance measurements from *Hall and Anderson* [1984] to develop a linear relationship between the solar irradiance at the center of the $Mg^+$ resonances and the $Mg^+$ (Mg II) index measured by SBUV. The Mg II index, as defined by *Heath and Schlesinger* [1986], is the ratio of the average solar flux measured by SBUV at the center of the Mg II Fraunhofer line to the average solar flux in the wings of the line. The Mg II index is approximately linearly related to both the 10.7-cm flux and sunspot number [*Heath and Schlesinger*, 1986]. Although the relationship between the solar irradiance at the $Mg^+$ resonance and the Mg II index is not precisely linear, we used a linear model because only a limited number of high-spectral-resolution balloon measurements were available (only four such measurements were obtained between 1978 and 1983). The linear relationship was extrapolated after 1983 to near-solar-minimum conditions.

Figure 3 shows the normalized solar irradiance at 2803 Å versus the Mg II index as computed by *Hall and Anderson* [1988]. Also shown is the derived linear relationship and extrapolation over the range of Mg II index values measured with SBUV. The absolute value of the solar irradiance at the $Mg^+$ resonances was derived by intercalibration of the balloon measurements with solar irradiance measurements from the Spacelab 2 solar ultraviolet spectral irradiance monitor (SUSIM) [L. A. Hall and G. P. Anderson, private communication, 1995]. Once the solar flux at the core of the Mg II resonance is determined, $g$ can be computed according to equation (3). Figure 4 shows the computed column emission rate, $g$, for the time period between 1979-1986 based on SBUV solar irradiance measurements. Also shown are representative error bars resulting from instrument noise. The daily variability in $g$, of the order of ±5%, is related to the solar rotational period. The 25% long-term decrease in $g$ is related to the 11-year solar cycle.

The standard deviation of the radiance error resulting from instrument noise at a given wavelength varies somewhat with solar zenith angle, with values of approximately 1% and 1.7% at low and high solar zenith angles, respectively. This results in estimated uncertainties in a single $Mg^+$ total column measurement of approximately 1.8 to 2.7 ions/cm$^2$ at high and low solar zenith angles, respectively. Bias in the derived column abundances will result from error in the absolute value of the solar flux at the $Mg^+$ resonance wavelength and systematic errors in the computed continuum (e.g., resulting from small calibration errors). The magnitude of the bias is difficult to estimate but could be as high as 50% or more. The effects of multiple scattering and self-absorption were neglected in computing column abundances from equation (2). These effects will be relatively small for our nadir-viewing geometry [*Gerard*, 1976; *Gerard et al.*, 1979]. The only effect of self-absorption on the derived column abundances will be at high solar zenith angles, where the optical depth may become large enough to affect the continuum. Owing to the Nimbus 7 orbit, high solar zenith angles (>80°) occur only at high latitudes. Therefore the column abundances reported here represent lower limits and may be underestimated at high latitudes.

## SBUV Observations and Comparisons With Previous Observations

$Mg^+$ dayglow near 2800 Å observed with SBUV represents emission from the entire vertical column. The normal atmosphere appears to have two layers of $Mg^+$ density enhancement: one relatively thin layer (full width at half maximum of approximately 2 km) near 93 km with a peak density of approximately 200 cm$^{-3}$ [*Aikin and Goldberg*, 1973] and a broad peak in the upper $E$ and $F$ regions at altitudes above 140 km. Altitude profiles of $Mg^+$ derived by *Fesen and Hays* [1982] show concentrations at altitudes between 300 and 475

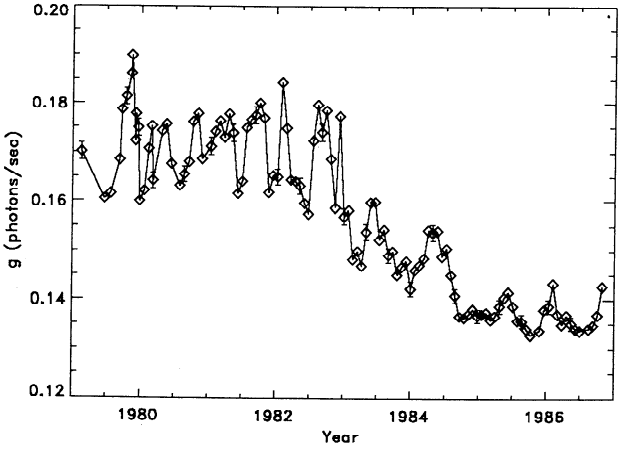


**Figure 4.** Column emission rate $g$ on observation days with representative error bars resulting from instrumental noise.

km near noon either approximately constant with altitude or falling off exponentially with altitude depending on latitude and longitude. The densities near noon at 300 km were relatively large, varying from approximately 50 to 100 $cm^{-3}$. Individual profiles are highly variable, so the profiles shown were averages over several months. These profiles were obtained during solar maximum conditions. Similar studies of the vertical distribution of $Mg^+$ by *Gerard et al.* [1979] show that near local noon between 140 and 190 km, the $Mg^+$ concentration is approximately constant (of the order of 100 $cm^{-3}$), falling off exponentially between 190 and 240 km with a scale height of approximately 25 km and continuing an exponential decrease above 240 km with a scale height of about 50 km. These results were obtained near solar minimum conditions. The lower altitude of the constant density region of the latter results as compared with the *Fesen and Hays* [1982] results is apparently related to the solar cycle as will be discussed later.

We evaluated the height integral in equation (2) for 50-km intervals starting at 90 km, using the densities obtained by *Aikin and Goldberg* [1973] below 120 km, a constant density of 10 $cm^{-3}$ between 120 and 140 km, and an approximate distribution from *Gerard et al.* [1979] above 140 km using a profile obtained near local noon. The maximum contribution to the total emission (approximately 40%) originates in the lower $F$ region at altitudes between 140-190 km, where the $Mg^+$ concentration is relatively constant with altitude. Approximately 7% of the emission originates from below 140 km. Of the remaining 53% of the total emission, approximately a third (or 18% of the total) originates from the 190 to 240-km layer and two thirds (or about 35% of the total) from above 240 km. Therefore the main contribution to the total emission results from $Mg^+$ in the upper $E$ and lower $F$ regions. Because the majority of the total column emission originates from the upper $E$ and $F$ regions, our derived total column abundances should compare favorably with previous upper $E$ and $F$ region metallic ion observations from mass spectrometers and limb-viewing spectrometers, although it should be noted that different quantities are being compared. Contribution to the observed emission from sporadic $E$ ($E_s$) layers, especially at midlatitudes, may be significant. Although $E_s$ layers occur over a narrow altitude range (approximately 1-2 km), the concentration of $Mg^+$ ions can reach values of the order of $10^4$ $cm^{-3}$ [e.g., *Gardner et al.*, 1993]. These concentrations would result in a column density of the order of $10^9$ $cm^{-2}$ through an $E_s$ layer that represents a significant fraction of the total column.

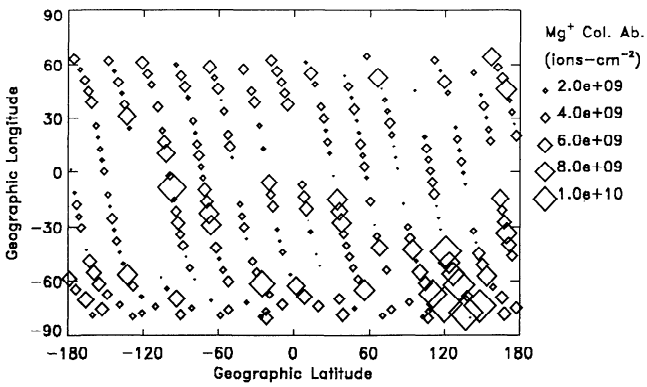


**Figure 5.** Observed $Mg^+$ total column abundance plotted in geographic coordinates on January 28, 1983, where the symbol size is proportional to the column abundance.

Figure 5 shows an example of derived $Mg^+$ column abundances on January 28, 1983, a magnetically quiet day. Although the spatial coverage on a single day is somewhat coarse and the signal-to-noise ratio is relatively low, patches of high column amounts of $Mg^+$ are observed. Observations from a space-shuttle-borne spectrometer showed poleward propagation of similar bright patches from metallic ion dayglow on successive orbits [*Gardner et al.*, 1994]. Averaging of many individual observations is required to infer information about dependent parameters because of the spatial inhomogeneity in $Mg^+$ column amounts and the relatively low signal-to-noise ratio.

Upper $E$ and $F$ region $Mg^+$ densities are expected to vary with magnetic activity [*Grebowsky and Brinton*, 1978] and solar sunspot activity [e.g., *Kumar and Hanson*, 1980; *Fesen et al.*, 1983; *Grebowsky and Pharo*, 1985]. In addition, variations in upper $E$ and $F$ region $Mg^+$ densities with dip latitude, longitude, and season at equatorial latitudes are expected to be coupled as a result of the longitude dependence of the position of the magnetic dip equator relative to the geodetic equator and ecliptic [e.g., *Grebowsky and Reese*, 1989]. Although these variations have been observed at specific altitudes, variations in the total column amount have not been previously shown. The following results show the variability in total $Mg^+$ column amounts as a function of these parameters as well as the coupling between them.

## Observed Variation With Magnetic Activity

Figure 6 shows the $Mg^+$ column abundance as a function of magnetic activity, separately, for low, middle, and high dip latitudes. Magnetic activity is quantified in terms of $C_9$, called the planetary daily character figure, derived by converting the commonly used $K_p$ index to a linear scale from 0 to 9 and averaging globally over a day. In Figure 6, $Mg^+$ column abundances are clearly enhanced with magnetic activity at all latitudes. Increases in $Fe^+$ occurrences with magnetic activity have been previously observed at high and middle latitudes between the 220- and 320-km altitude [*Grebowsky and Brinton*, 1978]. In order to ensure that the increase in the $Mg^+$ column in Figure 6 was not related to solar cycle effects that will be shown next, the variation in the $Mg^+$ total column with magnetic activity was examined under both solar maximum and solar minimum

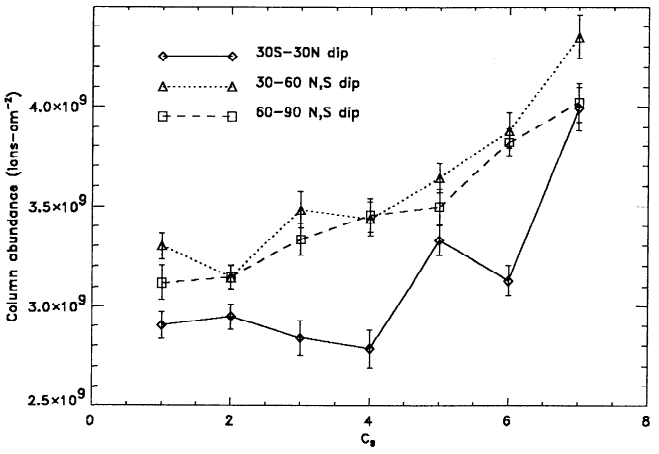


**Figure 6.** Observed $Mg^+$ column abundance versus $C_9$ (an indicator of magnetic activity) for three latitude bins with standard errors.

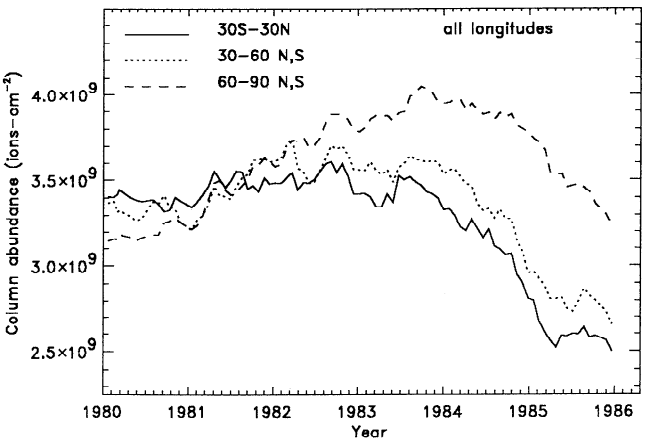


**Figure 8.** Similar to Figure 7, showing 25-point running averages of observed daily zonal mean $Mg^+$ column abundance for three latitude bins.

conditions and was found to be virtually identical in both cases.

## Observed Variation With Solar Cycle

Figure 7 shows the $Mg^+$ total column abundance averaged daily at latitudes between 30°S and 30°N as a function of time from 1979 to late 1986. Some of the scatter in the $Mg^+$ total column daily averages results from the effects of instrument noise. The daily variability of magnetic activity that affects $Mg^+$ column abundances, as shown above, also contributes to the observed daily variability. A 25-point running average applied to the daily averages is also shown in Figure 7. From mid-1982 to 1986, when solar sunspot activity was decreasing, $Mg^+$ column abundances at equatorial latitudes decrease by approximately 30-40%. Figure 8 shows smoothed daily averages as in Figure 7, separately, for low (<30°), middle (30°-60°), and high (>60°) latitudes. The largest decrease in the $Mg^+$ column density with decreasing solar cycle activity appears at low latitudes. At high latitudes, $Mg^+$ column amounts appear to peak later than at low and middle latitudes. Similar behavior in NO column amounts has been observed with SBUV during the same time period [*McPeters*, 1989]. Decreases in NO with decreasing solar activity were observed at low latitudes, and a similar peak in high-latitude NO was observed, where the peak occurred slightly later than the solar maximum peak.

In order to determine whether the 1982-1986 decrease is statistically significant, a regression analysis was performed for the three latitude bands in Figure 8. Daily averages of $Mg^+$ were regressed against the column emission rate $g$ that is proportional to solar chromospheric activity. The resulting fit at low latitudes is shown as a dashed line in Figure 7. Analysis of the regression indicates that the fit is statistically significant at low and middle dip latitudes. The probability of obtaining the correlation by chance, assuming that the variability is normally distributed and that the model is reasonable, was less than 0.01% for the low latitudes and less than 1% at middle latitudes.

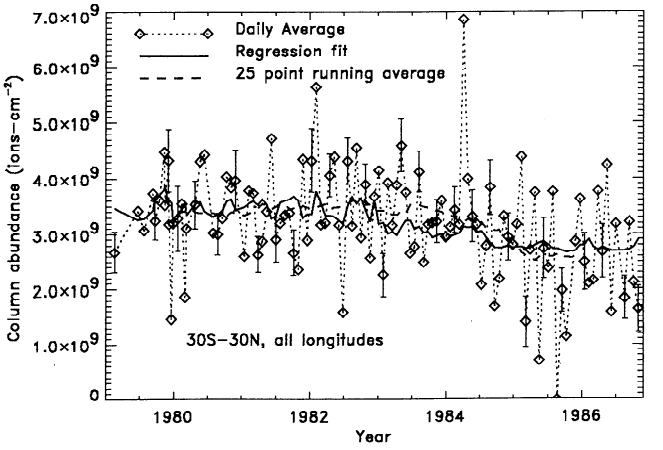


**Figure 7.** Observed daily zonal mean $Mg^+$ column abundance and representative errors with 25-point running average and regression fit, as explained in text.

## Observed Variation With Dip Latitude, Longitude, and Season

Figure 9 shows the seasonal variation in the $Mg^+$ total column as a function of dip latitude. The $Mg^+$ column abundance is averaged over the entire year and averaged over 6-month time periods centered around the June and December solstices. North-south asymmetry is clearly shown with the greatest seasonal variation at dip latitudes between 40° and 60°. The seasonal variation at midlatitudes is slightly larger in the northern hemisphere as compared with the southern hemisphere. Figures 10 and 11 show the $Mg^+$ column abundance as a function of day of the year for low, middle, and high dip latitudes, separately, in the northern and southern hemispheres, respectively. A 20-point running average was applied to daily mean $Mg^+$ column amounts. A peak in the $Mg^+$ column abundance is clearly shown

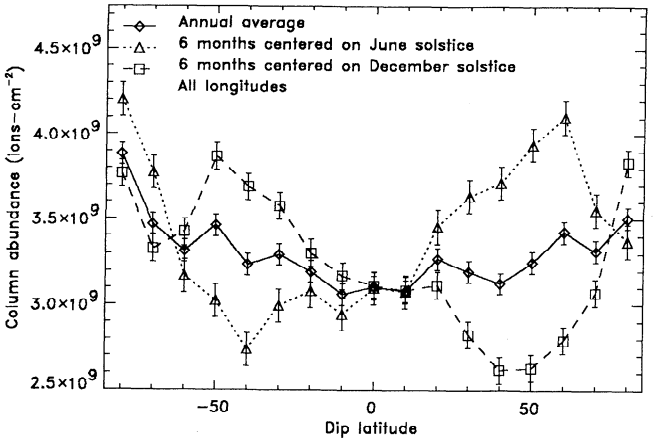


**Figure 9.** Observed $Mg^+$ column abundance binned as a function of dip latitude, for different time periods with standard errors.

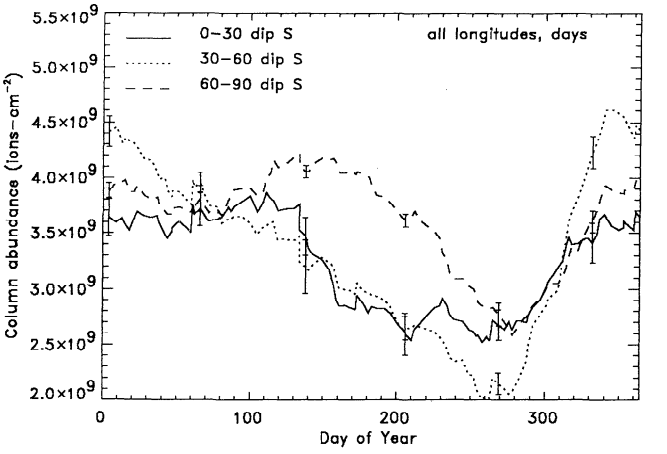


**Figure 11.** Same as Figure 10 but for southern hemisphere dip latitudes.

near the summer solstice at middle dip latitudes in the northern hemisphere. Less seasonal variability is observed at low and high dip latitudes in the northern hemisphere. A maximum and minimum in the $Mg^+$ total column are observed in the southern hemisphere, although they are shifted somewhat from the solstices. A somewhat stronger seasonal dependence at low and high latitudes is observed in the southern hemisphere as compared with the northern hemisphere. Similar seasonal variations in $Fe^+$ occurrences have been observed at midlatitudes between 220 and 320 km throughout the night until just before magnetic noon [*Grebowsky and Brinton*, 1978] and between 400 and 600 km during sunlit morning conditions [*Kumar and Hanson*, 1980].

Figures 12-14 show $Mg^+$ column abundances as a function of dip latitude averaged over four longitude sectors for the entire year and for the 6 months centered on the December and June solstices, respectively. In Figures 12 and 13, the lowest column densities are consistently observed in the 0-90°E sector. In Figure 14, maximum column densities are observed in the 90°-180°E sector during the northern summer, while lower densities are observed in the other three sectors. These figures show that the longitude dependence of total $Mg^+$ column is coupled with season. Although similar longitude variations in metallic ion occurrences, such as the low values in the 0-90°E sector, have been observed in the middle and upper $F$ regions [e.g., *Grebowsky and Reese*, 1989; *Kumar and Hanson*, 1980], the coupled longitude-seasonal variation has not been previously shown.

## Observed Neutral Mg Dayglow

It is more difficult to detect neutral Mg than $Mg^+$ with buv observations. The contrast between the resonance scattering signal and the continuum is lower at 2850 Å than at 2800 Å, owing to the higher continuum at 2850 Å. The initial analysis of excess emission at 2850 Å revealed no evidence of resonance scattering from neutral Mg. However, a close examination re-

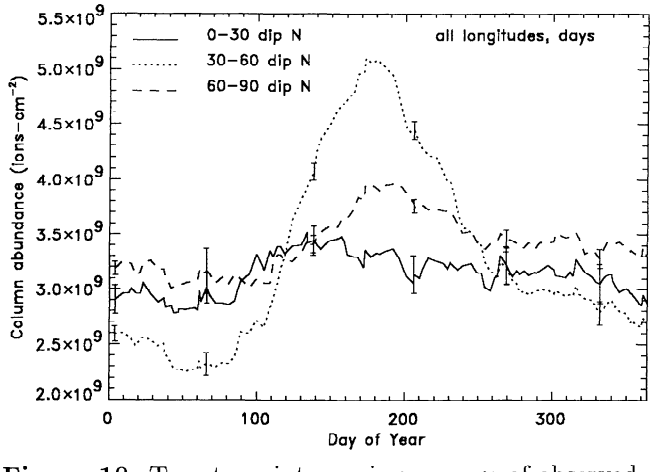


**Figure 10.** Twenty-point running average of observed daily zonal mean $Mg^+$ column abundances in the northern hemisphere as a function of day of the year with representative errors.

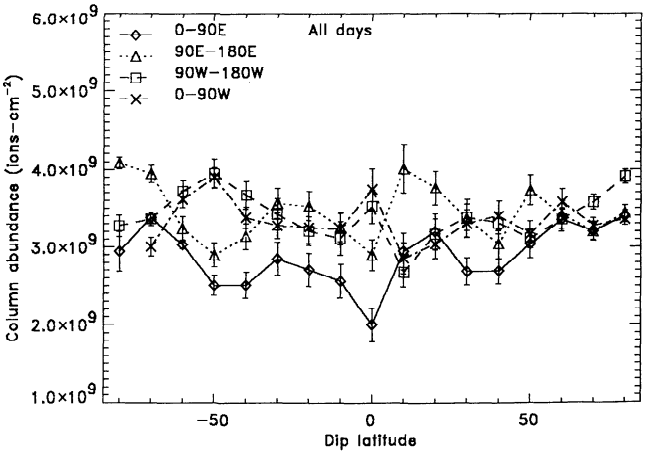


**Figure 12.** Observed $Mg^+$ column abundance binned as a function of dip latitude for four longitude sectors with standard errors.

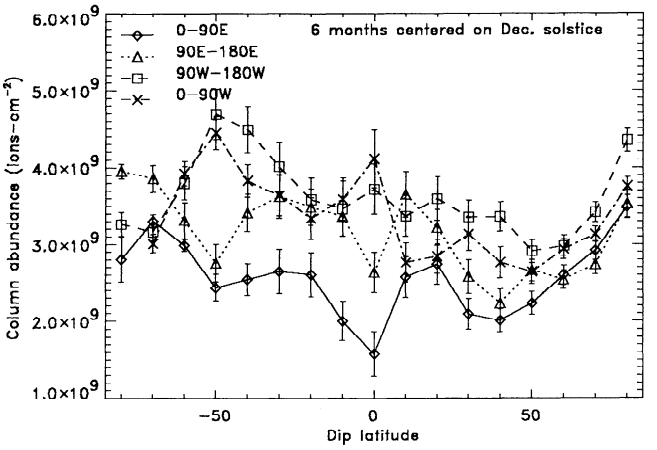


**Figure 13.** Same as Figure 12 but for 6 months centered on December solstice.

vealed possible resonance scattering from neutral Mg. A slight skew occurred in the distribution of the excess emission at 2850 Å about that expected from rotational-Raman scattering. There were approximately 100 observations, or less than 0.4%, when the excess radiance at 2850 Å was more than $3\sigma$ above that expected from rotational-Raman scattering. Approximately one third of the $+3\sigma$ observations are expected as the result of instrument noise on the basis of the statistics. In more than half the $+3\sigma$ observations, the large excess radiance occurred more than once on a single day, and the multiple observations occurred in close geographic proximity to one another. In these cases, the excess emission is attributed to neutral Mg resonance scattering. The average computed column density of the $+3\sigma$ observations is approximately $4\times10^{10}$ cm$^{-2}$.

The infrequent neutral Mg emission was not significantly correlated with strong $Mg^+$ emission. *Gardner et al.* [1994, 1995] detected infrequent neutral Mg emission, much smaller than $Mg^+$ emission, with a limb-viewing spectrometer at altitudes from 80 to 250 km. In contrast with our observations, the *Gardner et al.* [1994, 1995] Mg detections were correlated with strong $Mg^+$ emission. The small number of Mg observations prevents any detection of variation in the Mg abundance with meteor influx or any other parameters.

## Discussion

The total column of $Mg^+$ varies with magnetic activity, solar cycle activity, season, latitude, and longitude. The detailed chemical and dynamical modeling needed to quantitatively explain these variations is beyond the scope of this paper. Instead, we review the known processes that affect the production, destruction, and transport of Mg and $Mg^+$ in the ionosphere and describe qualitatively how these mechanisms may contribute to the observed variations in the $Mg^+$ total column.

The production mechanisms for $Mg^+$ are charge transfer with the major ionospheric ions ($NO^+$, $O_2^+$, and $O^+$) and direct photoionization. The loss process for $Mg^+$ in the upper $E$ and $F$ regions is the relatively slow radiative recombination with ionospheric electrons. At lower altitudes (90-100 km), $Mg^+$ is also removed by the three-body formation of $MgO_2^+$ and $MgO^+$ that recombines dissociatively to form neutral Mg. The mechanisms that transport $Mg^+$ upward from its $E$ region source to the $F$ region, where it can act as a passive tracer (lifetime > 1 day), depend on latitude and altitude [e.g., *MacLeod et al.*, 1975].

Several mechanisms related to electric and magnetic fields produce vertical transport of $Mg^+$, from the source in the $E$ region to higher altitudes. At low latitudes, ions can be lifted vertically from the source region by Pedersen drifts associated with the vertical polarization dynamo $E$ field. At middle and high latitudes, fast upward Pedersen ion drifts associated with intense electric fields can raise ions from the source region into the $F$ region [*Grebowsky and Pharo*, 1985]. In the $F$ region, one of the major transport processes results from $\mathbf{E} \times \mathbf{B}$ drift that produces both vertical and horizontal transport.

Several other transport mechanisms are associated with thermospheric neutral winds. At low altitudes (lower $E$ region), collisional interactions dominate transport, producing vertical and horizontal motion of both Mg and $Mg^+$. Another form of transport in the $E$ region is vertical motion produced by zonal neutral wind motion across horizontal magnetic field lines and is associated with sporadic $E$ layers. At higher altitudes in the $F$ region, neutral winds with a component parallel to magnetic field lines can raise or lower ions along field lines, depending on the wind direction and inclination.

### Magnetic Activity Dependence

Magnetic activity has the effect of increasing column amounts of $Mg^+$ at all latitudes, as illustrated in Figure 6. Therefore the total amount of $Mg^+$ is greater dur-

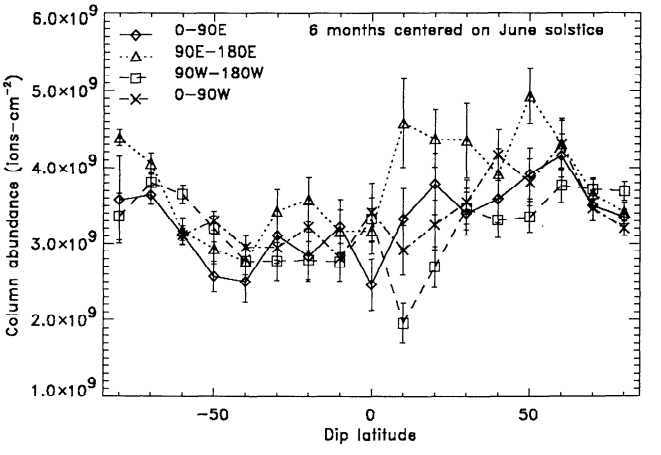


**Figure 14.** Same as Figure 13 but for 6 months centered on June solstice.

ing periods of high magnetic activity than when magnetic activity is low. Several factors may contribute to enhanced production and transport of $Mg^+$ during magnetically disturbed conditions. Ionization changes are associated with magnetic activity [*Rishbeth et al.*, 1985; *Hagan*, 1988; *Fesen et al.*, 1989]. Increased ion densities increase $Mg^+$ production through charge exchange. Vertical transport of $Mg^+$ increases during periods of high magnetic activity. Enhanced auroral heating associated with magnetic activity can cause vertical upwelling at high latitudes that would raise ions. During magnetically disturbed conditions, fast upward Pedersen ion drifts produced by intense $E$ fields can raise metallic ions from their $E$ region source into the $F$ region in the afternoon and during the night primarily at high and middle latitudes [*Grebowsky and Pharo*, 1985]. Enhanced auroral heating during periods of high magnetic activity at high latitudes can produce an equatorward wind at night [*Mayr and Hedin*, 1977] that can raise ions at midlatitudes owing to its component along field lines. Once ions are raised from their source region at night by the latter two mechanisms, they can be held in the $F$ region until early afternoon by the dawn expansion of the $F$ region plasma [*Grebowsky and Brinton*, 1978]. At low latitudes, possible coupling between high-latitude magnetic activity and equatorial electric fields [*Nopper and Carovillano*, 1978] may enhance vertical motion via Pedersen drifts to raise ions out of their source region. Because our observations are made only 1 day per month and periods of high magnetic activity sometimes extend over several days, the time evolution of the enhancement of $Mg^+$ cannot be accurately measured. Observations with improved temporal and vertical resolution are needed to better understand the effects of magnetic activity on metallic ion distributions.

### Solar Cycle Dependence

In Figure 8, significant decreases are observed in the total column $Mg^+$ from the solar sunspot maximum period in 1979-1983 to the solar sunspot minimum period in 1984-1986, especially at low and middle latitudes. Our measurements differ from previous metallic ion measurements across the solar cycle in several respects. Previously, information from different sensors on different orbiting platforms was used to infer solar cycle effects on metallic ion distributions [e.g., *Kumar and Hanson*, 1980]. In contrast, our data were obtained with the same instrument, and the results are relatively insensitive to calibration drift. Previous metallic ion observations were obtained at specific altitude ranges, in contrast with the total column abundances reported here. Our total column measurements indicate that the total amount of $Mg^+$ in the atmosphere increases with increasing solar activity.

Previous observations [e.g., *Kumar and Hanson*, 1980] have shown an increase in the occurrence of metallic ions with solar activity primarily above 200 km. These observations were attributed in part to greater (lesser) vertical drifts and magnitudes of electric fields (that induce vertical transport) associated with the solar sunspot maximum (minimum). *Fesen et al.* [1983] modeled low-latitude $Mg^+$ densities for both solar minimum and solar maximum conditions. For altitudes from the 125-km model boundary to approximately 600 km, $Mg^+$ densities were the same or enhanced at solar maximum as compared with solar minimum. The region of constant $Mg^+$ density extended over a greater range of altitudes at solar maximum. The $Mg^+$ enhancement during solar maximum was attributed to increases in vertical transport, solar 10.7-cm flux, and the oxygen photoionization rate. No comment was made regarding total column $Mg^+$ variation with solar activity, although estimating the total column density from their reported number densities indicates that under almost all simulated conditions, the total column of $Mg^+$ is greater at solar maximum. It is possible that some of the observed increase in total column $Mg^+$ with solar cycle activity arises from variations at low altitudes resulting from increased production of $Mg^+$. Increased production of $Mg^+$ is expected at solar maximum as the result of the increased photoionization rate of both Mg and the major ions with which Mg charge exchanges.

### Coupled Seasonal, Latitude, and Longitude Effects

Several effects may contribute to the observed maximum (minimum) in the $Mg^+$ column at midlatitudes in summer (winter), as observed in Figures 9-11. Production of $Mg^+$ is greater in the summer hemisphere owing to increased ionization of Mg and major ions. Upward vertical transport is increased in the summer hemisphere compared with the winter hemisphere as the result of several mechanisms. Upward vertical diffusion of both neutral Mg and $Mg^+$ is enhanced in the summer hemisphere at midlatitudes [e.g., *Roble and Kasting*, 1984]. The summer hemisphere predawn equatorward wind raises ions along field lines from the $E$ region to the lower $F$ region. Then, the morning upward expansion of the $F$ region can raise ions farther into the $F$ region and hold them there until late morning or early afternoon [*Grebowsky and Brinton*, 1978] when our observations are made. In winter, the opposite effect takes place; that is, the predawn neutral wind blows poleward, pushing ions down field lines and preventing them from reaching the topside $F$ region.

*Kane and Gardner* [1993] reported a seasonal variation in the neutral Fe column abundance of $\pm$ 50% at midlatitudes measured with ground-based lidar. This seasonal variation in neutral Fe is anticorrelated with the seasonal variation in $Mg^+$ reported here; that is, a minimum (maximum) in the neutral Fe column was observed in the summer (winter). The summer minimum in Fe was explained by a chemical model in which colder summer mesospheric temperatures produce an increase in the reaction rate to form the sink molecule $FeCO_3$. Transport was not accounted for in this chemical model,

but was acknowledged as a potentially important factor in determining the metallic neutral/ion equilibrium. If a correlation between Fe and Mg exists (neutral and ionic) and the chemistries are similar, which appears to be the case [e.g., *Aikin and Goldberg*, 1973], some of the observed decrease (increase) in summer neutral (ion) column abundances could be related to increased upward transport. This effect would increase (decrease) the metallic ion to neutral ratio in the summer (winter), because the reactions to form the neutral from the ion depend on the square of the atmospheric density and the $O_3$ concentration.

The interpretation of the longitude dependence of $Mg^+$ column densities and the longitude dependence of the dip latitude asymmetry is problematic, in that there are several possible explanations or combinations thereof that cannot be confirmed or rejected on the basis of our observations. There are several possible longitude-dependent mechanisms that affect vertical transport. The longitude-dependent mechanisms likely vary with time of day as well as altitude, so that our measurements are not necessarily comparable with previous observations, although some similarities between our total column observations and previous observations at specific altitudes and different times of day were found to exist.

Vertical drifts at low altitudes depend on the relative positions of the magnetic dip equator and geodetic equator. The longitudinal dependence of total column $Mg^+$ observations appears to be related to the longitude dependence of the position of the geomagnetic equator relative to the geographic equator. For longitudes west (east) of the Greenwich meridian, the dip equator is generally south (north) of the geomagnetic equator. Total column $Mg^+$ amounts in the west longitude sectors are generally enhanced over those at east longitudes for the 6 months centered on the December solstice, although not at all latitudes. There is somewhat of a reversal of this effect for the 6-month averages centered on the June solstice, although again, not at all latitudes. The seasonal behavior of the longitude dependence is probably related to the variation of the dip equator with respect to the ecliptic plane, as suggested by *Grebowsky and Reese* [1989].

Zonal winds with a dip equatorward component can drag ions along field lines. This effect would cause the north-south asymmetry in upper $E$ and $F$ region $Mg^+$ densities to vary with declination that depends on longitude. Metallic ion observations of *Kumar and Hanson* [1980] at night at altitudes about 100 km were consistent with an eastward wind after sunset, when the most frequent ion detections were made. Our total column observations, however, do not appear to be simply related to a constant direction zonal wind. *Kumar and Hanson* [1980] could not rule out the possibility of a longitudinal variation in the $\mathbf{E} \times \mathbf{B}$ drift (although no evidence for this has been given) or injection of rising large-scale plasma depletions or bubbles that contain metal ions as the cause of the longitudinal dependence of observed $F$ region metallic ions. Similarly, we cannot rule out these possibilities.

## Conclusions

We have shown that backscattered ultraviolet measurements provide a useful tool for studying metallic ion column behavior in the upper atmosphere. Our SBUV observations definitively show that total column $Mg^+$ amounts increase with solar cycle activity at low and middle latitudes, increase with magnetic activity at all latitudes, and increase in summer at midlatitudes. The global total column measurements reported here are complementary to previous $E$ and $F$ region studies of metallic ion distributions. The observations can be qualitatively explained in terms of chemistry and transport mechanisms. Chemistry-transport modeling is needed to understand the relative importance of the processes that affect metallic ion total column densities.

The examination of data from other satellite buv instruments, such as the SBUV/2 instruments flying aboard National Oceanic and Atmospheric Administration operational satellites, may provide further information about the behavior of metallic ions in the upper atmosphere. These instruments could produce similar snapshots of $Mg^+$ total column abundances potentially at different times of day. Future buv instruments with higher spectral and temporal resolution will provide an improved diagnostic tool for study of the thermosphere and ionosphere.

**Acknowledgments.** The authors wish to thank L. A. Hall and G. P. Anderson for providing calibrated high-resolution solar irradiance data. They also thank K. S. Noll, J. M. Grebowsky, R. D. McPeters, R. P. Cebula, J. F. Gleason, and E. G. Stassinopoulos for valuable discussions and comments.

The editor thanks C. G. Fesen and another referee for their assistance in evaluating this paper.

## References

Aikin, A. C., and R. A. Goldberg, Metallic ions in the equatorial ionosphere, *J. Geophys. Res.*, *78*, 734-745, 1973.

Anderson, J. G., and C. A. Barth, Rocket investigation of the Mg I and Mg II dayglow, *J. Geophys. Res.*, *76*, 3723-3732, 1971.

Fesen, C. G., and P. B. Hays, $Mg^+$ morphology from visual airglow experiment observations, *J. Geophys. Res.*, *87*, 9217-9223, 1982.

Fesen, C. G., P. B. Hays, and D. N. Anderson, Theoretical modeling of low-latitude $Mg^+$, *J. Geophys. Res.*, *88*, 3211-3223, 1983.

Fesen, C. G., G. Crowley, and R. G. Roble, Ionospheric effects at low latitudes during the March 22, 1979, geomagnetic storm, *J. Geophys. Res.*, *94*, 5405-5417, 1989.

Gardner, C. S., T. J. Kane, D. C. Senft, J. Qian, and G. C. Papen, Simultaneous observations of sporadic $E$, Na, Fe, and $Ca^+$ layers at Urbana, Illinois: Three case studies, *J. Geophys. Res.*, *98*, 16,865-16,873, 1993.

Gardner, J. A., R. A. Viereck, E. Murad, S. T. Lai, D. J.

Knecht, C. P. Pike, A. L. Broadfoot, E. R. Anderson, and W. J. McNeil, $Mg^+$ and other metallic emissions observed in the thermosphere, *Proc. SPIE, 2266*, 242-252, 1994.

Gardner, J. A., R. A. Viereck, E. Murad, D. J. Knecht, C. P. Pike, A. L. Broadfoot, and E. R. Anderson, Simultaneous observations of neutral and ionic magnesium in the thermosphere, *Geophys. Res. Lett., 22*, 2119-2122, 1995.

Gerard, J.-C., Satellite measurements of high-altitude twilight $Mg^+$ emission, *J. Geophys. Res., 81*, 83-87, 1976.

Gerard, J.-C., and A. Monfils, Satellite observations of the equatorial Mg II dayglow intensity distribution, *J. Geophys. Res., 79*, 2544-2550, 1974.

Gerard, J.-C., and A. Monfils, The Mg II equatorial airglow altitude distribution, *J. Geophys. Res., 83*, 4389-4391, 1978.

Gerard, J.-C., D. W. Rusch, P. B. Hays, and C. L. Fesen, The morphology of equatorial $Mg^+$ ion distribution deduced from 2800-Å airglow observations, *J. Geophys. Res., 84*, 5249-5258, 1979.

Grebowsky, J. M., and H. C. Brinton, $Fe^+$ ions in the high-latitude $F$ region, *Geophys. Res. Lett., 5*, 791-794, 1978.

Grebowsky, J. M., and M. W. Pharo III, The source of mid-latitude metallic ions at $F$-region altitudes, *Planet. Space Sci., 33*, 807-815, 1985.

Grebowsky, J. M., and N. Reese, Another look at equatorial metallic ions in the $F$ region, *J. Geophys. Res., 94*, 5427-5440, 1989.

Hagan, M. E., Effects of geomagnetic activity in the winter thermosphere, 2, Magnetically disturbed conditions, *J. Geophys. Res., 93*, 9937-9944, 1988.

Hall, L. A., and G. P. Anderson, Solar ultraviolet variation between 1977 and 1983, *J. Geophys. Res., 89*, 7322, 1984.

Hall, L. A., and G. P. Anderson, Instrumental effects on a proposed Mg II index of solar activity, *Ann. Geophys., 6*, 531-534, 1988.

Hanson, W. B., D. L. Sterling, and R. F. Woodman, Source and identification of heavy ions in the equatorial $F$ layer, *J. Geophys. Res., 77*, 5530-5541, 1972.

Heath, D. F., and B. M. Schlesinger, The Mg 280-nm doublet as a monitor of changes in solar ultraviolet irradiance, *J. Geophys. Res., 91*, 8672-8682, 1986.

Heath, D. F., A. J. Kruger, H. A. Roeder, and B. D. Henderson, The solar backscatter ultraviolet and total ozone mapping spectrometer (SBUV/TOMS) for Nimbus G, *Opt. Eng., 14*, 323-331, 1975.

Joiner J., P. K. Bhartia, R. P. Cebula, E. Hilsenrath, R. D. McPeters, and H. Park, Rotational-Raman scattering (Ring effect) in satellite backscatter ultraviolet measurements, *Appl. Opt., 34*, 4513-4525, 1995.

Kane, T. J., and C. S. Gardner, Structure and seasonal variability of the nighttime mesospheric Fe layer at midlatitudes, *J. Geophys. Res., 98*, 16,875-16,886, 1993.

Kumar, S., and W. B. Hanson, The morphology of metallic ions in the upper atmosphere, *J. Geophys. Res., 85*, 6783-6801, 1980.

MacLeod, M. A., T. J. Keneshea, and R. S. Narcisi, Numerical modeling of a metallic ion sporadic $E$, *Radio Sci., 10*, 371, 1975.

Mayr, H. G., and A. E. Hedin, Significance of large-scale circulation in magnetic storm characteristics with application to AE-C neutral composition data, *J. Geophys. Res., 82*, 1227-1234, 1977.

McPeters, R. D., Climatology of nitric oxide in the upper stratosphere, mesosphere, and thermosphere: 1979 through 1986, *J. Geophys. Res., 94*, 3461-3472, 1989.

Mende, S. B., G. R. Swenson, and K. L. Miller, Observations of $E$ and $F$ region $Mg^+$ from Spacelab 1, *J. Geophys. Res., 90*, 6667-6673, 1985.

Narcisi, R. S., Mass spectrometer measurements in the ionosphere, in *Physics and Chemistry of the Upper Atmosphere*, p. 171, D. Reidel, Hingham, Mass., 1973.

Noll, K. S., M. A. McGrath, L. M. Trafton, S. K. Atreya, J. J. Caldwell, H. A. Weaver, R. V. Yelle, C. Barnet, and S. Edginton, HST spectroscopic observations of Jupiter after the collision of comet Shoemaker-Levy 9, *Science, 267*, 1307-1313, 1995.

Nopper, R. W., Jr., and R. L. Carovillano, Polar-equatorial coupling during magnetically active periods, *Geophys. Res. Lett.*, 5, 699-702, 1978.

Park, H., D. F. Heath, and C. L. Mateer, Possible application of the Fraunhofer line filling in effect to cloud height measurements, in *Meteorological Optics, OSA Tech. Dig. Ser.*, pp. 70-81, Opt. Soc. Am., Washington, D. C., 1986.

Rishbeth, H., R. Gordon, D. Rees, and T. J. Fuller-Rowell, Modeling of thermospheric composition changes caused by a severe magnetic storm, *Planet. Space Sci., 33*, 1283-1301, 1985.

Roble, R. G., and J. F. Kasting, The zonally averaged circulation, temperature, and compositional structure of the lower thermosphere and variations with geomagnetic activity, *J. Geophys. Res., 89*, 1711-1724, 1984.

Schlesinger, B. M., R. P. Cebula, D. F. Heath, and A. J. Fleig, Nimbus 7 solar backscatter ultraviolet (SBUV) spectral scans solar irradiance and Earth radiance product user's guide, *NASA Ref. Publ., 1199*, 1988.

Wiese, W. L., M. W. Smith, and B. M. Glennon, Atomic transition probabilities, in *Hydrogen Through Neon*, vol. 1, Nat. Bur. of Stand., Washington, D. C., 1966.

A. C. Aikin and J. Joiner, Laboratory for Atmospheres, NASA Goddard Space Flight Center, Code 910.3, Greenbelt, MD 20771 (e-mail:aikin@chapman.gsfc.nasa.gov; joiner@dao.gsfc.nasa.gov)

(Received June 22, 1995; revised October 23, 1995; accepted November 15, 1995.)